Hindawi
Advances in Materials Science and Engineering
Volume 2018, Article ID 7390798, 13 pages
https://doi.org/10.1155/2018/7390798

*Research Article*

# A Comparative Experimental Study on the Flexural Behavior of High-Strength Fiber-Reinforced Concrete and High-Strength Concrete Beams

**In-Hwan Yang**[1], **Changbin Joh**[2] **and Kyoung-Chul Kim**[3]

[1]*Professor, Kunsan National University, Department of Civil Engineering, Kunsan, Jeonbuk 54150, Republic of Korea*
[2]*Research Fellow, Korea Institute of Civil Engineering and Building Technology, Structural Engineering Research Institute, Goyang, Gyeonggi 10223, Republic of Korea*
[3]*Senior Engineer, DM Engineering, Department of Structural Engineering, Seoul 05288, Republic of Korea*

Correspondence should be addressed to In-Hwan Yang; ihyang@kunsan.ac.kr

Received 19 March 2018; Revised 28 June 2018; Accepted 30 July 2018; Published 4 September 2018

Academic Editor: Wen Deng



The flexural responses of high-strength fiber-reinforced concrete (HSFRC) beams and high-strength concrete (HSC) beams are compared in this study. A series of HSFRC and HSC beams were tested under pure flexural loading. The effects of the type of concrete, compressive strength of the concrete, and tensile rebar ratio on the flexural behavior of the concrete beams were investigated. The flexural behavior of the HSFRC and HSC beams including the induced crack and failure patterns, load and deflection capacity, crack stiffness, ductility index, and flexural toughness was compared. The crack stiffness of the HSC and HSFRC beams increased with the rebar ratio. For the same rebar ratios, the crack stiffness of the HSFRC beams was much greater than that of the HSC beams. The ductility index of the HSC beams decreased sharply with an increase in the rebar ratio, but the ductility index of the HSFRC beams did not show a clear decrease with increasing rebar ratio. The flexural toughness of the HSFRC beams was greater than that of the HSC beams at higher rebar ratios of 1.47% and 1.97%, indicating that the energy absorption of the HSFRC beams was greater than that of the HSC beams. Test results also indicated that HSFRC developed better and more consistent ductility with higher rebar ratio. In addition, the tested bending strength and sectional analysis results were compared.

## 1. Introduction

Compared to conventional concrete, high-strength concrete (HSC) develops higher compressive strength along with improved durability, ductility, and high elastic modulus that have recently promoted its extended application to many structures [1–3]. For example, Min et al. [4] investigated the shrinkage characteristics of high-strength concrete for large underground space structures to explore what ingredient in the mixture affected these characteristics. Ho et al. [5] evaluated analytically the effectiveness of adding confinement for ductility improvement of HSC columns. They concluded that the use of HSC could reduce the size of columns at the cost of some reduction in the flexural ductility of the columns.

Many tests have been performed to evaluate the flexural behavior of HSC beam specimens [6–9]. The results of Ashour [8] showed that the flexural rigidity increased with greater compressive strength of the concrete. The test results of Mohammadhassani et al. [10] showed that an increase in tensile rebar ratio improved the ultimate load capacity but decreased the deflection ductility index. The ductility index is thus significantly influenced by the rebar ratio. Compared with normal-strength concrete, the increased compressive strength of HSC makes it more brittle and less resistive to crack opening and propagation. Therefore, the tensile reinforcement of HSC beams is important for controlling the deflection of the beams and the crack formation within the beams.

The addition of steel fibers can increase the ductility, fracture toughness, and loading capacity of concrete members [11, 12]. High-strength fiber-reinforced concrete (HSFRC) is an advanced cement composite material reinforced with steel fiber and has a limited porosity for

a concrete matrix. In HSFRC, steel fiber is an important factor affecting both the mechanical properties and structural capacity of concrete members [13–16]. Several studies on the flexural behavior of HSFRC beams have been conducted [17–20]. Chunxiang and Patnaikuni [18] investigated the effects of different steel fibers on the flexural behavior of beams. They concluded that the addition of steel fibers significantly improved the flexural performance, including the bending strength and deflection capacity. To examine the influence of steel fiber on the flexural behavior of HSFRC members, Su et al. [19], Guan et al. [20], and Mertol et al. [21] conducted studies with different volume dosages of steel fiber. They reported that the bearing capacity of HSFRC increased with the steel fiber volume dosage. In addition, a flexural analysis of ultra-high-performance concrete beams, which can be regarded as a kind of HSFRC, was suggested by Chen and Graybeal [22], Bae et al. [23], and Ning et al. [24].

However, most experimental studies on the flexural behavior of HSC and HSFRC were performed on either HSC beams or HSFRC beams. There are few direct comparison studies on experimental results of HSFRC beams and HSC beams, which have almost the same concrete compressive strength. To enhance the understanding of the difference between the flexural behavior of HSFRC beams and that of HSC beams, an experimental investigation is needed.

Therefore, this study intends to compare the characteristics of the flexural behavior of HSC and HSFRC beams that have nearly identical concrete compressive strengths. The test parameters include the compressive strength of the concrete and tensile rebar ratio of the concrete beams. The compressive strengths of 100 MPa and 120 MPa are considered, and the tensile rebar ratios of 0.98%, 1.47%, and 19.7% are used in this study. The comparison of the flexural behavior of the HSFRC beams and HSC beams is done in terms of the crack and failure patterns, crack stiffness, bending capacity, and ductility. Finally, a comparison of the sectional analysis and experimental results of the bending strength is performed.

## 2. Experimental Program

*2.1. Mixture Proportions of the HSC and HSFRC.* In this study, three mixing proportions, H100, H120, and HF120, were used to fabricate test beams, as shown in Table 1. The three-digit numbers in each mixture name represented the target compressive strength of the concrete. The H100 and H120 mixtures were used to fabricate the HSC beams, while the HF120 mixture was used to fabricate the HSFRC beams.

The H100 and H120 mixtures had low water-binder ratios of 0.2 and 0.15 to attain the high compressive strength of concrete. The cement used in these two mixtures was ordinary Portland cement (OPC). Blast furnace slag (BFS) and silica fume (SF) were also used as binders in the H100 and H120 mixtures. Coarse aggregates with a maximum size of 20 mm and a density of 2.6 g/cm$^3$ were included in the H100 and H120 mixtures, and sand was used as fine aggregate.

The HF120 mixture did not include coarse aggregates but did include zirconium and 1% steel fibers by volume of concrete. Richard and Cheyrezy [11] suggested that limiting the coarse aggregates in the mixture could create a homogenous and dense cementitious matrix. In addition, coarse aggregates were excluded in the HF120 mixture to limit microcrack formation in the interface zone between the coarse aggregate and cementitious matrix. Crushed quartz with an average diameter of 10 $\mu$m and a density of 2,600 kg/m$^3$ was used as a filler material in the HF120 mixture. The steel fibers used in this study were straight and had a diameter of 0.2 mm and length of 19.5 mm, as shown in Figure 1. The density of the steel fiber was 7,500 kg/m$^3$, and its yield strength was 2,500 MPa.

Conventional concrete usually includes only OPC as binder. However, additionally to OPC, HSFRC in this study also included blast furnace slag, silica fume, and zirconium as binders, as well as filler and steel fiber. Therefore, the HSFRC was about five times more expensive than the conventional concrete.

Compared with laboratory specimens, the structural members actually used onsite have larger length and sectional dimensions, and it also takes more time to complete the placing of HSFRC. It may thus be more difficult to control the workability and flow of HSFRC onsite than in laboratory condition. The placing method and workability of the HSFRC mixture influence sensitively the orientation and distribution of steel fibers and consequently affect the mechanical properties of HSFRC. Therefore, the difficulty in achieving workability and flow should be considered for structural applications because the large dimension and placing time delay of HSFRC may cause significant variation in the mechanical properties of concrete.

*2.2. Material Properties.* The compressive strengths of the HSFRC and HSC were obtained through compressive testing on cylindrical specimens. Three concrete mixtures with different compressive strengths were used in this study. The mean compressive strengths of the H100, H120, and HF120 cylindrical specimens were 96.9, 118.3, and 135.5 MPa, respectively, as shown in Table 2. The measured compressive strengths of the H100 and H120 specimens almost reached the target compressive strengths of 100 and 120 MPa. However, the measured compressive strength of the HF120 specimen was greater than its target compressive strength of 120 MPa. After the compressive strength test, the relationship between the stress and strain of each specimen was obtained to compute the compressive strength and elastic modulus, as shown in Figure 2. The mean elastic moduli of the H100, H120, and HF120 specimens were 37511, 38623, and 39192 MPa, respectively, as shown in Table 2.

Five $100 \times 100 \times 400$ mm prenotched prismatic specimens were fabricated from each batch to determine the tensile strength of the HSFRC. A three-point bending test on a prenotched prism was used to obtain the tensile strength of the HSFRC [25]. A notch was cut into the tensile zone, and a clip gauge was attached at the notch to measure the crack mouth opening displacement (CMOD). The load-CMOD

Table 1: Mixing proportions.

| Mixture | W/B | W (kg/m$^3$) | OPC (kg/m$^3$) | BFS (kg/m$^3$) | SF (kg/m$^3$) | Zr (kg/m$^3$) | S (kg/m$^3$) | F (kg/m$^3$) | G (kg/m$^3$) | Steel fiber ($V_f$) (%) |
|---|---|---|---|---|---|---|---|---|---|---|
| H100 | 0.2 | 165.0 | 557.5 | 165.0 | 82.5 | — | 571.1 | — | 792.4 | — |
| H120 | 0.15 | 150.0 | 700.0 | 150.0 | 150.0 | — | 467.5 | — | 765.1 | — |
| HF120 | 0.22 | 209.0 | 770.0 | 135.0 | — | 58.0 | 847.0 | 231.0 | — | 1.0 |

*Note*. W: water; B: binders; OPC: ordinary Portland cement; BFS: blast furnace slag; SF: silica fume; Zr: zirconium; S: sand; F: filler; G: coarse aggregate.

Figure 1: Steel fiber used for the HSFRC mixture (HF120).

curves of notched specimens are shown in Figure 3. Based on the measured load-CMOD relationship curve, an inverse analysis was performed to estimate the tensile strength of the HSFRC. The inverse analysis procedure followed that of Yang et al. [17], using the measured load-CMOD relationship. The mean tensile strength of the HF120 mixture prismatic specimens was 7.8 MPa, as shown in Table 2.

In this study, a high-strength reinforcement bar (rebar) with a nominal diameter of 16 mm (D16) was used to reinforce the HSFRC and HSC beam specimens. The mean yield strengths of the rebar used in the H100, H120, and HF120 series beams were 607.9, 595.8, and 670.0 MPa, respectively, as shown in Table 2.

*2.3. Details of the Structural Test Specimen and Instrumentation.* To understand the flexural behavior of HSFRC and HSC beams, a total of 9 beam specimens were fabricated and tested. The cross section of the beams was rectangular with a beam width of 200 mm and a beam height of 250 mm, and the overall length of the beams was 3,300 mm. The dimensions and reinforcement details of the beams are shown in Figure 4. To avoid shear failure, all the specimens were reinforced by stirrups with a diameter of 10 mm at a spacing of 150 mm. The stirrups were used only in the shear spans, but they were not included in the 600 mm long constant moment region. The main parameters in the test program were the type of concrete (HSC and HSFRC), compressive strength of the concrete, and rebar ratio, as shown in Table 2. Two types of concrete beams, namely, HSC and HSFRC beams, were cast with different rebar ratios, which ranged between 0.98 and 1.97%. Two target concrete compressive strengths of 100 and 120 MPa were considered.

All the specimens were tested by using the four-point loading method. The load was applied using a hydraulically operated actuator and transferred from the actuator to the beam through a spread beam. The beams were set on a pair of steel supports with a clear span of 3,000 mm. The distance from the load to the middle of the constant moment zone was 300 mm. Each beam test was conducted under displacement control at a constant speed of 1.5 mm/min.

To measure the deflection that occurred during the loading, three LVDTs were placed under the constant moment region of the beam. The beam specimens were supported by roller supports as usually done the four-point loading test of beams. Therefore, horizontal LVDT was not included to measure potential support movement in the instrumentation plan. The strain of both the concrete and steel rebar was measured by electrical resistance strain gauges. Four strain gauges were attached to the steel rebar, and five strain gauges were mounted on the side of the beam at midspan, as shown in Figure 5.

## 3. Experimental Results

*3.1. Crack and Failure Patterns.* The crack and failure patterns of the HSFRC and HSC beams are shown in Figure 6. The initial cracking of the HSC and HSFRC beams occurred in the constant moment region. However, the cracks propagated more deeply into the compressive zone in the HSC beam than in the HSFRC beam. This result shows that the steel fibers in the HSFRC beams arrested the crack propagation. After an initial crack occurred, new cracks formed, and the widths of the existing cracks continued to enlarge with the load in both the HSFRC and HSC beams. At yield load and maximum load, more cracks formed in the HSFRC beams than in the HSC beams. Here, the yield load, that is the load at rebar yielding, was monitored by strain gauges attached to the rebar, and the maximum load was identified on the load-deflection curve of test beam.

In addition, the crack width in the HSC beams was larger than that in the HSFRC beams. These results indicate that the addition of steel fibers affected the width of the cracks in the HSFRC beams. Steel fibers played a role in bridging the cracks and redistributing the stress in the HSFRC beams, allowing more cracks to form in the HSFRC beams compared to the HSC beams.

The typical failure of the HSC members occurred by a sudden crushing of the concrete in the compressive zone, while the typical failure of the HSFRC beams resulted from the steel fiber pulling out of the HSFRC matrix. The measurement of the load and crack width relationship is shown in Figure 7. The crack widths in the HSFRC beams were smaller than those in the HSC beams at the same load level, up to the yielding of the rebar. For example, at the yield load of the H100-R1 beam (78 kN), the crack width of the HF120-R1 beam was 0.15 mm while the values of the H100-R1 and

Table 2: Details of the beam specimens.

| Beam specimens | Concrete type | Beam section | | Concrete | | | Rebar | | | | |
|---|---|---|---|---|---|---|---|---|---|---|---|
| | | Width (mm) | Height (mm) | Compressive strength $f'_c$ (MPa) | Elastic modulus $E_c$ (MPa) | Tensile strength $f_t$ (MPa) | Nominal diameter (mm) | Number of rebars | Yielding strength $f_y$ (MPa) | Area of rebar $A_s$ ($mm^2$) | Rebar ratio ($\rho$) (%) |
| H100-R1 | HSC | 200 | 250 | | | | 16 | 2 | 607.9 | 397.2 | 0.98 |
| H100-R2 | HSC | 200 | 250 | 96.9 | 37,511 | — | 16 | 3 | 607.9 | 595.8 | 1.47 |
| H100-R3 | HSC | 200 | 250 | | | | 16 | 4 | 607.9 | 794.4 | 1.97 |
| H120-R1 | HSC | 200 | 250 | | | | 16 | 2 | 595.8 | 397.2 | 0.98 |
| H120-R2 | HSC | 200 | 250 | 118.3 | 38,623 | — | 16 | 3 | 595.8 | 595.8 | 1.47 |
| H120-R3 | HSC | 200 | 250 | | | | 16 | 4 | 595.8 | 794.4 | 1.97 |
| HF120-R1 | HSFRC | 200 | 250 | | | | 16 | 2 | 670.0 | 397.2 | 0.98 |
| HF120-R2 | HSFRC | 200 | 250 | 135.5 | 39,192 | 7.8 | 16 | 3 | 670.0 | 595.8 | 1.47 |
| HF120-R3 | HSFRC | 200 | 250 | | | | 16 | 4 | 670.0 | 794.4 | 1.97 |

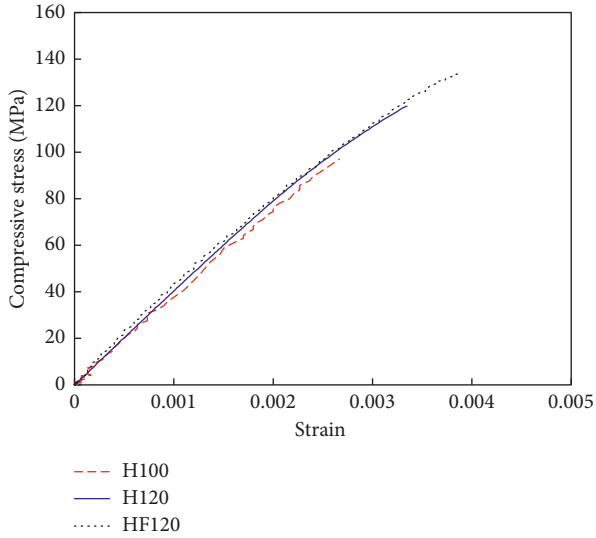


Figure 2: Compressive stress-strain curves.

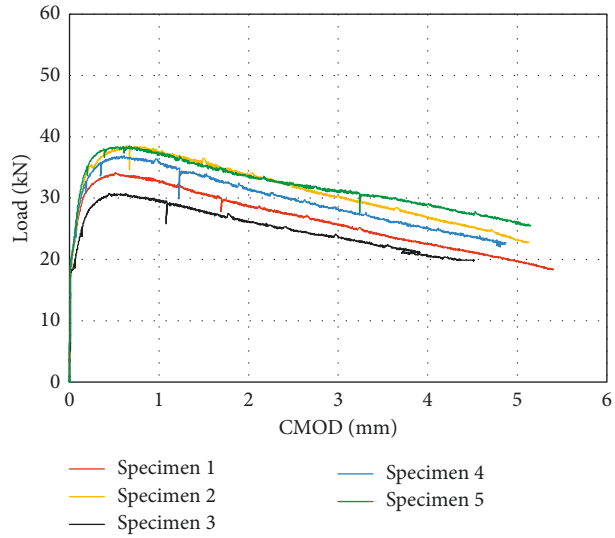


Figure 3: Load-CMOD relationship curves.

H120-R1 beams were 1.2 and 0.4 mm, respectively. For the rebar ratio of 1.47% (R2), at the yield load of the H100-R2 beam (129 kN), the H100-R2 and H120-R2 exhibited the crack widths of 0.8 and 1.73 mm, respectively, while the HF120-R2 had hairline cracks with the width of 0.2 mm. Similarly, at the yield load of the H100-R3 beam (129 kN), the H100-R3 and H120-R3 beams exhibited crack widths larger by 3.6 and 4.3 times, respectively, compared with the HF120-R3 beam. This result indicates that the steel fibers in the HSFRC beams affected the crack behavior.

In the HSFRC beams, after the load reached the peak load, the width of one crack increased suddenly and developed into a major crack. The major crack of the HSFRC beam occurred at the bottom of the beam and propagated upward to the compressive zone. Because the steel fibers resisted the opening of the crack, the major crack widened with the increase in the load until the fibers were pulled out of the matrix. Thus, the width of the major crack in the HSFRC members was clearly wider than the widths of the other cracks.

*3.2. Load-Deflection Relationship.* The load-deflection curves of the HSC and HSFRC beams with various rebar ratios are shown in Figure 8. The test results show that the bending strength of both the HSC beams and HSFRC beams increased with the rebar ratio. For the H120 series beams, the maximum loads of the H120-R2 and H120-R3 beams increased, respectively, by 32.4% and 71.2% compared with that of the H120-R1 beam. For the HF120 series beams, the maximum loads of the HF120-R2 and HF120-R3 beams increased, respectively, by 23.9% and 58.6% compared with that of the HF120-R1 beam. These results show that the maximum load of the HSC beams underwent greater increase rate with higher rebar ratio than that of the HSFRC beams.

The test results also show that the deflection of the HSC beams at the maximum load decreased with the increase in the rebar ratio. For the H100 series beams, at the maximum load, the deflection of the H100-R1 beam was greater than that of the H100-R2 and H100-R3 beams. For the H120 series beams, at the maximum load, the deflection of the H120-R1 beam was also greater than that of the H120-R2 and H120-R3 beams. However, in contrast, the deflection of the HSFRC beams at the maximum load increased with the rebar ratio. At the maximum load, the deflection of the

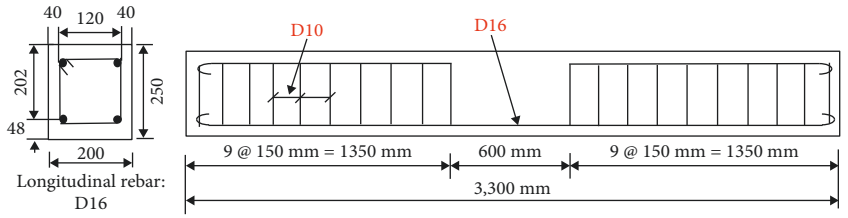


Figure 4: Dimensions of the beams.

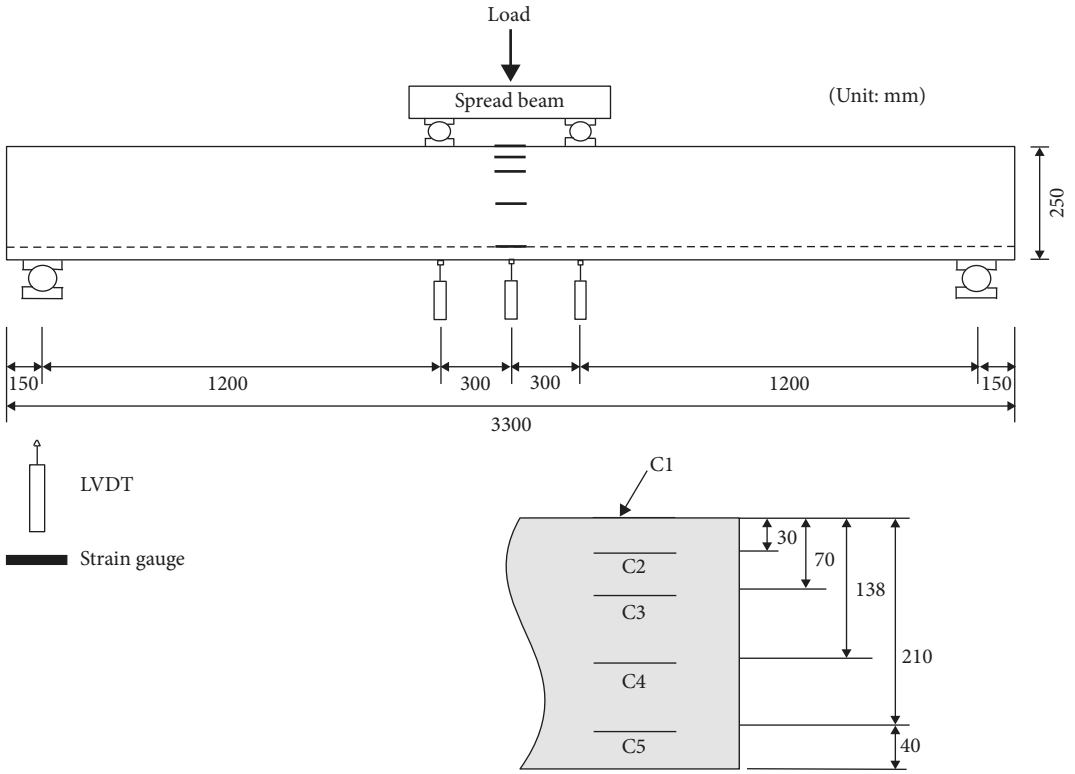


Figure 5: Instrumentation used for the flexural tests of the beams.

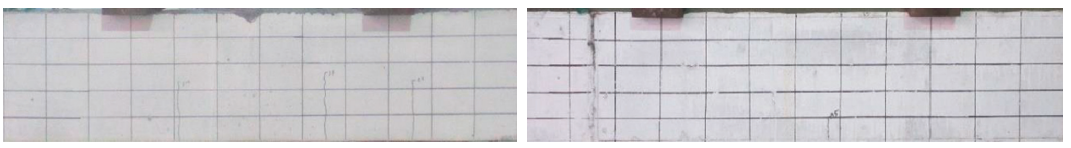

H120-R2 beam HF120-R2 beam

(a)

H120-R2 beam HF120-R2 beam

(b)

Figure 6: Continued.

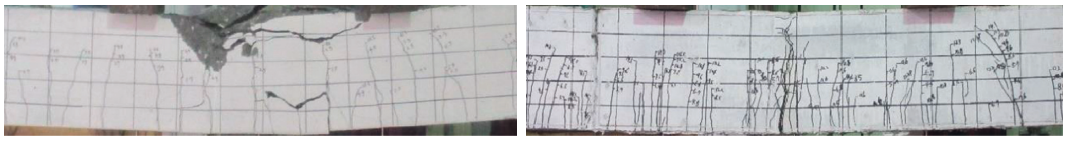

H120-R2 beam HF120-R2 beam

(c)

Figure 6: Crack and failure patterns of the HSC and HSFRC beams. (a) Initial cracking state. (b) Yielding state. (c) Ultimate state.

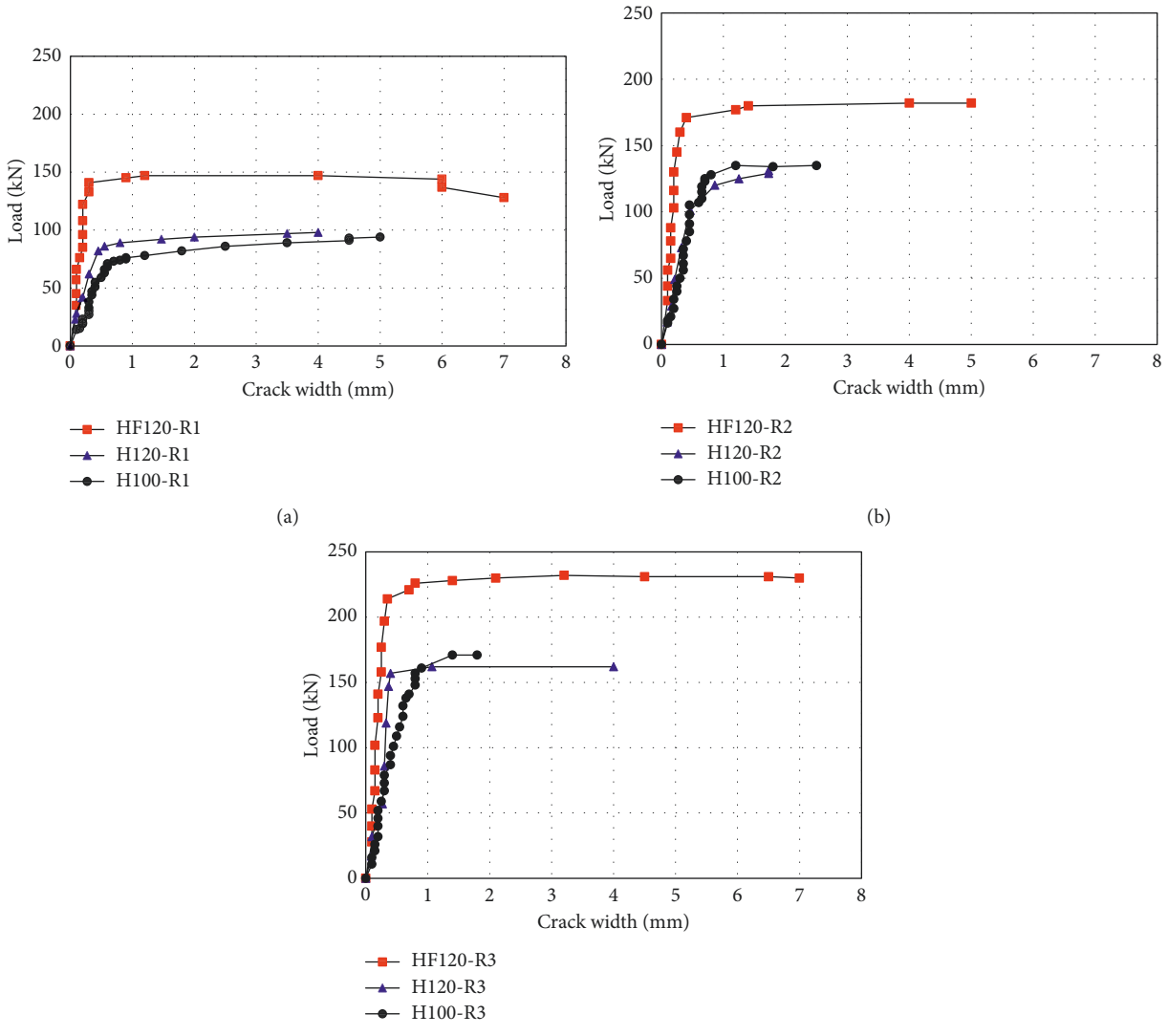


Figure 7: Load and crack width relationship. (a) Rebar ratio of 0.98%. (b) Rebar ratio of 1.47%. (c) Rebar ratio of 1.97%.

HF120-R3 beam was greater than those of the HF120-R1 and HF120-R2 beams.

The load-deflection curves of the test beams with different types of concrete are shown in Figure 9. The maximum load of the H100 series beams and that of the H120 series beams did not show a significant difference at the same rebar ratio. These results indicate that the compressive strength had little influence on the flexural behavior of the test beams. However, the maximum loads of the HSFRC beams were much greater than those of the HSC beams due to the contribution of the steel fiber to the bending strength of the HSFRC beams. Additionally, use of HSFRC improved the bending strength of the beams remarkably.

The test results also show that the deflection capacity of the HSFRC beam at the failure of the beam increased with the increase in rebar ratio. For the rebar ratio of 0.98% (R1), the deflection at the failure of the HF120-R1 beam was less than that of the two other beam types, as shown in

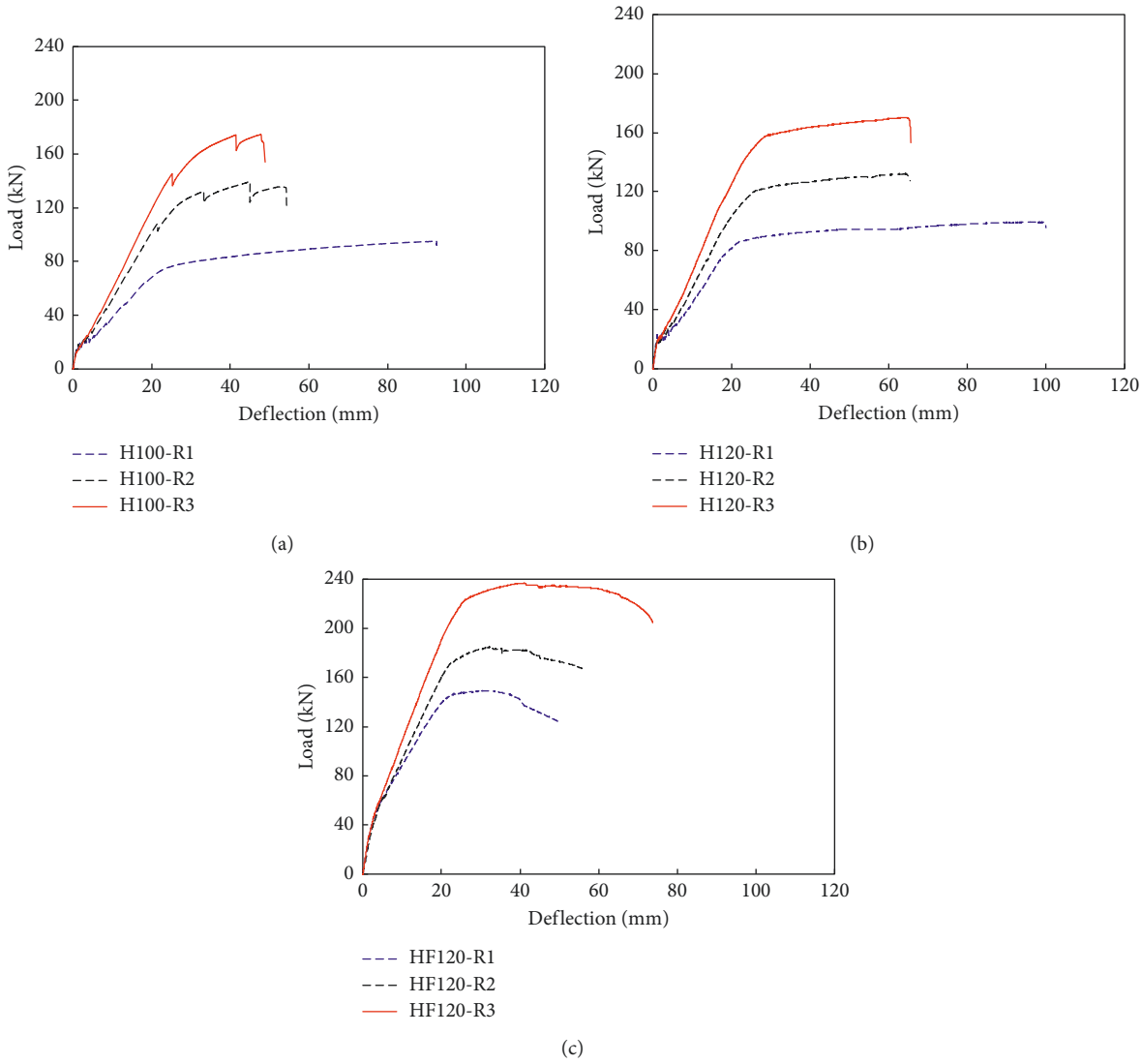


Figure 8: Load-deflection curves at different rebar ratios. (a) H100 series beams. (b) H120 series beams. (c) HF120 series beams.

Figure 9(a). For the rebar ratio of 1.47% (R2), the deflection at the failure of the HF120-R2 beam was similar to that of the two comparison beams, as shown in Figure 9(b). However, for the rebar ratio of 1.97% (R3), the deflection at the failure of the HF120-R3 beam was greater than that of the two comparison beams, as shown in Figure 9(c).

*3.3. Crack Stiffness.* The stiffness of a concrete beam drops after the initiation of the first crack because the contribution of the concrete to the stiffness of the beam is reduced in the cracked section. Thus, the crack stiffness of the beams was investigated in this study. The crack stiffness is calculated by the following equation [26].

$$K_{cr} = \frac{P_y - P_{cr}}{\Delta_y - \Delta_{cr}}, \quad (1)$$

where $K_{cr}$ is the crack stiffness, $P_y$ is the yield load, $P_{cr}$ is the cracking load, $\Delta_y$ is the deflection corresponding to the yield load, and $\Delta_{cr}$ is the deflection corresponding to the cracking load.

The crack stiffness of each series of concrete beams is shown in Table 3 and Figure 10. For each type of concrete, the crack stiffness of the concrete beam increased with the rebar ratio. The crack stiffnesses of the H100-R1, H100-R2, and H100-R3 beams were 2.35, 3.82, and 4.71 kN/mm, respectively. The crack stiffnesses of the H120 beams were slightly higher, and their corresponding indices were 3.00, 4.11, and 5.09 kN/mm, respectively.

However, under the condition of the same rebar ratio, the crack stiffness of the HF120 series beams was much greater than those of the H100 and H120 series beams. The crack stiffness of the HF120-R1, HF120-R2, and HF120-R3 beams was 5.09, 6.23, and 7.59 kN/mm, respectively. In particular, the crack stiffness of the HF120-R1 beam was 2.2 and 1.7 times greater than those of the H100-R1 and H120-R1 beams, respectively. The crack stiffness of the HF120-R2 beam was also greater by 1.63 and 1.52 times than those of

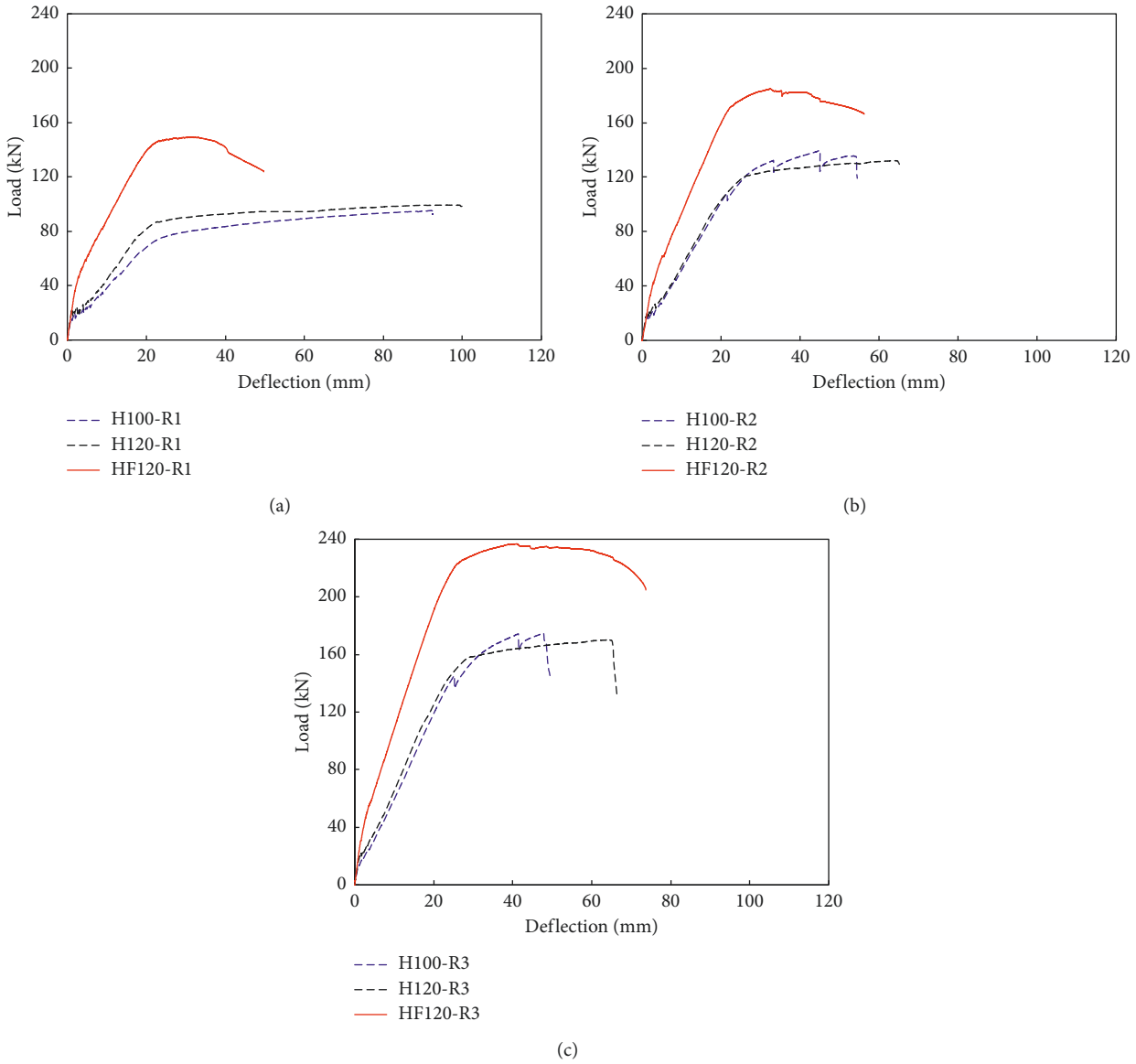


Figure 9: Load-deflection curves for different types of concrete. (a) Rebar ratio of 0.98%. (b) Rebar ratio of 1.47%. (c) Rebar ratio of 1.97%.

Table 3: Experimental results of the beam specimens.

| Beam specimens | Initial cracking state | | | Yielding state | | | Peak state | | | Crack stiffness | Ductility index | Flexural toughness | Normalized flexural toughness |
|---|---|---|---|---|---|---|---|---|---|---|---|---|---|
| | $P_{cr}$ (kN) | $M_{cr}$ (kN) | $\Delta_{cr}$ (mm) | $P_y$ (kN) | $M_y$ (kN) | $\Delta_y$ (mm) | $P_p$ (kN) | $M_p$ (kN) | $\Delta_p$ (mm) | $K_{cr}$ (kN/mm) | | (kN·mm) | (kN·mm) |
| H100-R1 | 16.1 | 9.6 | 0.9 | 78.0 | 46.8 | 27.3 | 95.3 | 57.2 | 92.1 | 2.35 | 3.38 | 6,980 | 6,980 |
| H100-R2 | 16.4 | 9.8 | 1.0 | 129.0 | 30.5 | 30.5 | 139.6 | 83.8 | 45.0 | 3.82 | 1.47 | 5,224 | 5,224 |
| H100-R3 | 12.7 | 7.6 | 0.9 | 162.0 | 32.6 | 32.6 | 174.6 | 104.8 | 47.8 | 4.71 | 1.47 | 5,641 | 5,641 |
| H120-R1 | 23.3 | 14.0 | 1.2 | 86.4 | 51.8 | 22.2 | 99.4 | 59.6 | 96.1 | 3.00 | 4.34 | 8,065 | 8,229 |
| H120-R2 | 17.4 | 10.4 | 0.9 | 120.4 | 72.2 | 26.0 | 131.6 | 79.0 | 60.9 | 4.11 | 2.35 | 6,482 | 6,614 |
| H120-R3 | 17.4 | 10.4 | 1.0 | 157.2 | 94.3 | 28.5 | 170.2 | 102.1 | 64.5 | 5.09 | 2.26 | 8,230 | 8,397 |
| HF120-R1 | 46.4 | 27.8 | 2.9 | 145.1 | 87.1 | 22.3 | 149.3 | 89.6 | 30.5 | 5.09 | 1.37 | 5,456 | 4,950 |
| HF120-R2 | 62.2 | 37.3 | 5.1 | 172.4 | 103.4 | 22.8 | 185.0 | 111.0 | 32.5 | 6.23 | 1.43 | 8,087 | 7,337 |
| HF120-R3 | 58.8 | 35.3 | 4.2 | 222.0 | 133.2 | 25.7 | 236.8 | 142.1 | 41.0 | 7.59 | 1.60 | 13,971 | 12,676 |

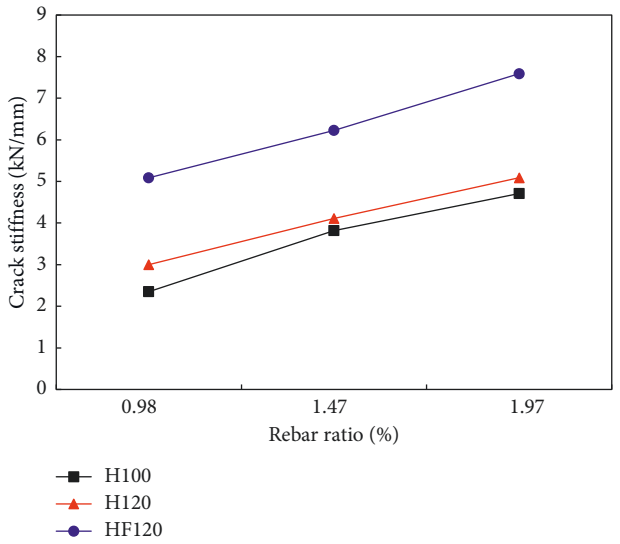


Figure 10: Crack stiffness of the HSFRC and HSC beams.

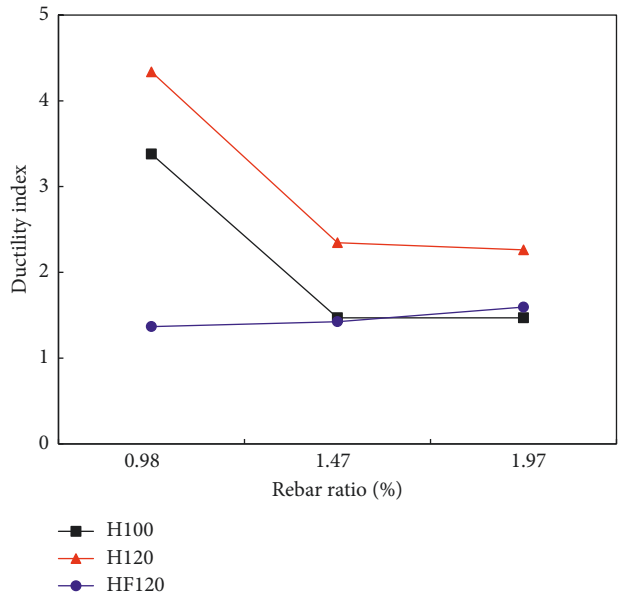


Figure 11: Ductility index of the HSC and HSFRC beams.

the H100-R2 and H120-R2 beams, respectively. Therefore, the test results show that the use of HSFRC significantly improved the crack stiffness of the concrete beams.

*3.4. Ductility.* The deflection at the midspan of each test beam was measured during the bending tests and used to calculate the ductility index. The ductility of the beam was calculated by Equation (2), which was suggested by Singh et al. [27].

$$\mu = \frac{\Delta_p}{\Delta_y}, \tag{2}$$

where $\mu$ is the ductility index, $\Delta_p$ is the deflection of the beam at the maximum (peak) load, and $\Delta_y$ is the deflection of the beam at the yield load.

The ductility indices are shown in Table 3 and Figure 11. This figure shows the ductility indices of the HSC series beams significantly decreased as the rebar ratio increased from 0.98 to 1.47% and decreased slightly or approximately remained the same as the rebar ratio increased from 1.47 to 1.97%. The ductility indices of the H100-R1, H100-R2, and H100-R3 beams were 3.38, 1.47, and 1.47, respectively. Additionally, the ductility indices of the H120-R1, H120-R2, and H120-R3 beams were 4.34, 2.35, and 2.26, respectively.

In contrast, the ductility of the HSFRC beams slightly improved in value and consistency with the rebar ratio. The ductility indices of the HF120-R1, HF120-R2, and HF120-R3 beams were 1.37, 1.43, and 1.60, respectively. The ductility indices of the HSFRC in this study ranged from 1.37 to 1.60, and those of ultra-high-performance concrete beams in a previous study [28] ranged from 1.31 to 1.99. This indicates that the ductility indices range of the HSFRC in this study was similar to that of the ultra-high-performance concrete. Additionally, the test results show that the ductility indices of the HSFRC beams were lower than those of the HSC beams, especially at low rebar ratios.

*3.5. Flexural Toughness.* The addition of steel fiber to concrete can improve the postcracking response of the concrete beam. Flexural toughness, which is a measure of the energy absorption capacity of the concrete beam, was calculated for each beam in this study. The flexural toughness was measured from the area under the load-deflection curve obtained from the bending test. The load-deflection curves shown in Figure 8 were used to estimate the flexural toughness of each beam.

Flexural toughness is affected by the strengths of concrete and rebar. The yield strengths of the rebar used in each series beam were different from each other. The flexural toughness of the H120 and HF120 series beams was normalized against that of the H100 series beams, which reflected the different yield strengths of the adopted rebar. The normalized flexural toughness was calculated by the following equation:

$$\mathrm{FT}_{\mathrm{normalized}} = \mathrm{FT} \times \frac{f_{y,\mathrm{H100}}}{f_y}, \tag{3}$$

where $\mathrm{FT}_{\mathrm{normalized}}$ is the normalized flexural toughness, $f_{y,\mathrm{H100}}$ is the yield strength of rebar used in the H100 series beams, and $f_y$ is the yield strength of rebar used in test beams.

The flexural toughness values of the HSC and HSFRC beams are shown in Table 3 and Figure 12. At the low rebar ratio of 0.98%, the normalized flexural toughness of the HSC beam was greater than that of the HSFRC beam. The normalized flexural toughness of the HF100-R1 and HF120-R1 beams was greater than that of HF120-R1 beam, by 41.0% and 66.2%, respectively.

The normalized flexural toughness of the HSFRC beams increased rapidly with the rebar ratio. However, the normalized flexural toughness of the HSC beams decreased with the increase in the rebar ratio from 0.98 to 1.47% and increased slightly with the rebar ratio from 1.47% to 1.97%.

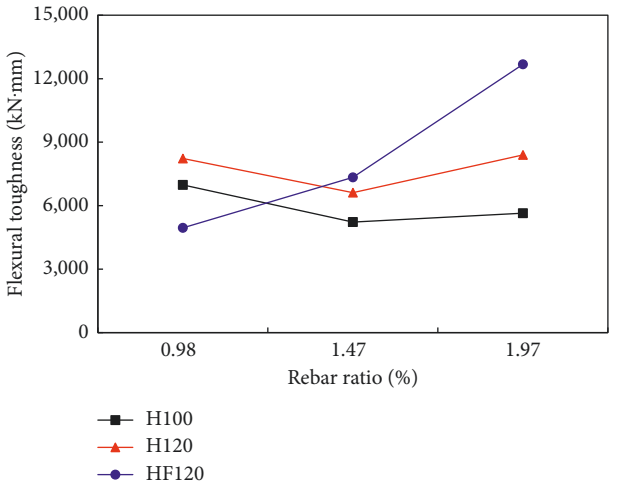


Figure 12: Normalized flexural toughness of the HSC and HSFRC beams.

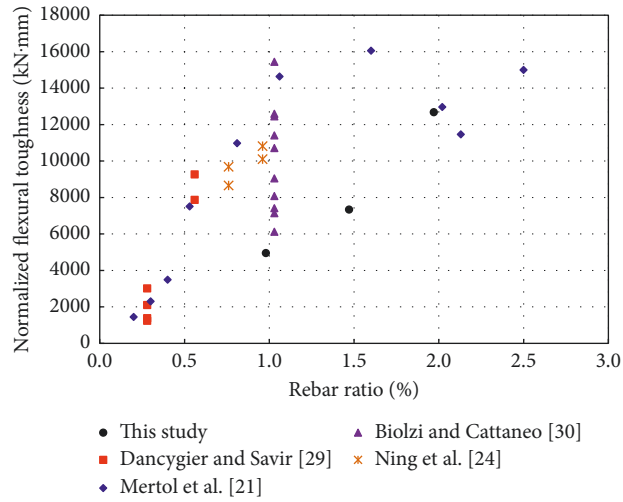


Figure 13: Comparison of the experimental results of flexural toughness for the HSFRC beams of this study and of previous studies.

The test results show that the flexural toughness of the HSC beams, compared with that of the HSFRC beams, was not affected significantly by rebar ratios between 0.98% and 1.97%.

The normalized flexural toughness of the HSFRC beams was greater than that of the HSC beams at the higher rebar ratios of 1.47% and 1.97%. In particular, the normalized flexural toughness of the HF120-R3 beam was 2.24 and 1.51 times greater than that of the HF100-R3 and HF120-R3 beams, respectively. These results indicate that the energy absorption in the HSFRC beams was greater than that of the HSC beams and that the application of HSFRC at higher rebar ratios would be effective to improve the flexural toughness of concrete structures.

In addition, the experimental results of flexural toughness for the HSFRC beams of this study and those for the similar HSFRC beams of previous studies [21, 24, 29, 30] are compared in Figure 13. It appears that the normalized flexural toughness of the HSFRC beams increased with the rebar ratio, and that, similarly to other studies, the normalized flexural toughness increased with the rebar ratio in this study.

## 4. Sectional Analysis of the Bending Moment-Curvature Relationship

Finite element analysis can be used to predict the structural performance of the concrete beams. The finite element method allows detailed visualization of the stresses and displacements and gives insight into the design parameters. However, it takes a lot of effort and time to get finite element solutions for structural analysis. Sectional analysis was applied to predict the moment-curvature relationship in this study. The moment-curvature relationship was calculated for the experimental beams. The analysis approach was based on the bending beam theory and modification of the commonly used sectional model by considering constitutive law of materials.

To predict the bending strengths of the H100, H120, and HF120 beams, moment-curvature curve analysis was performed. Sectional analysis was applied to predict the moment-curvature relationship. The strain and stress distributions along the beam depth is shown for a section in Figure 14. The cross section is divided into several layers by applying the multilayer method. The compression and tensile strains are assumed to be linear throughout the cross section. The compression and tensile strain of the section can be calculated by using the assumed curvature and neutral axis depth for each analytical step.

The strain distribution at the cross section is dependent on the neutral axis position for the assumed curvature. After determining the strain distribution, the stress distribution at the section can be obtained. The stress in each layer is calculated by using the stress-strain relationship of the concrete. The compressive stress-strain relationship of both the HSC and HSFRC was obtained from the compression tests for each type of concrete, as shown in Figure 2. The compressive stress-strain relationships of both the HSC and HSFRC were measured to be approximately linear. In addition, the compressive stress-strain relationship of both the HSC and HSFRC was modeled as a linear relationship, while the compressive stress-strain relationship for normal-strength concrete was modeled as a parabolic relationship. The compressive stress-strain relationship model of concrete for the HSC and the HSFRC is shown in Figure 15. The tensile stress-strain relationship of the HSFRC was obtained from the CMOD test results and inverse analysis, incorporating the load-CMOD curve. The tensile stress-strain relationship of the HSFRC was modeled with a linear elastic relationship and a softening relationship, as suggested by the Association Française de Génie Civil (AFGC) design recommendations [31]. The tensile stress-strain relationship of rebar was obtained from the tension test. The bilinear model shown in Figure 16 was used for rebar.

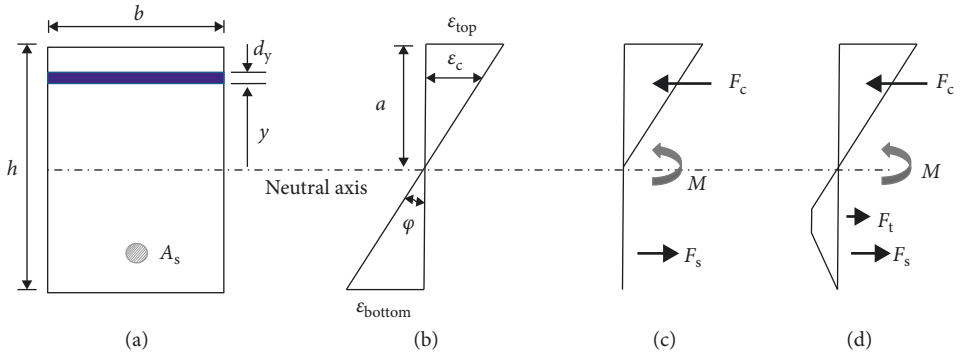


Figure 14: Strain and stress distributions in the section: (a) cross section; (b) strain distribution; (c) stress distribution of HSC; (d) stress distribution of HSFRC.

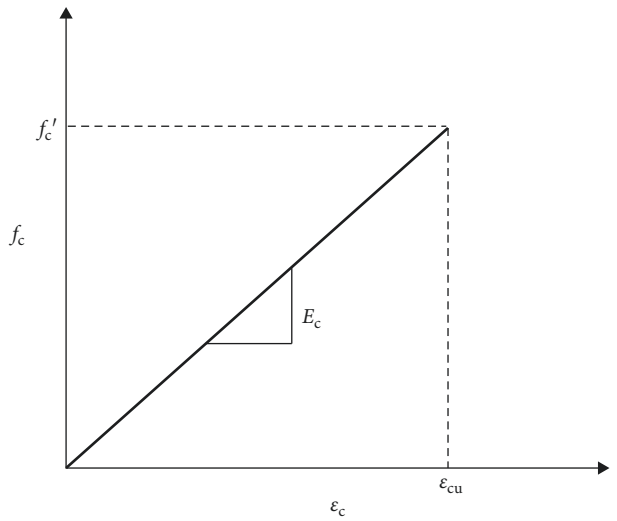


Figure 15: Compressive stress-strain relationship model of concrete for HSC and HSFRC.

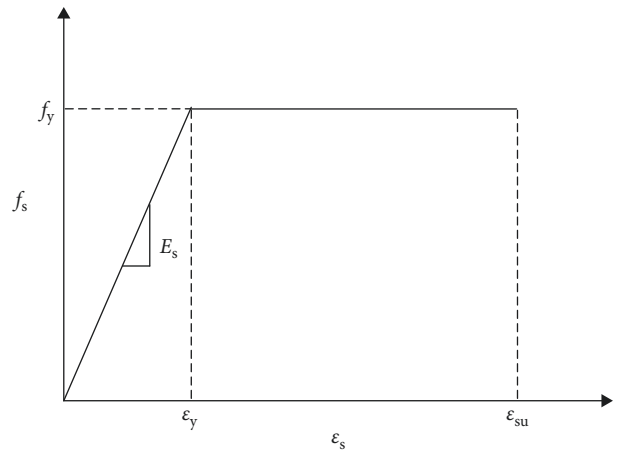


Figure 16: Tensile stress-strain relationship model of rebar.

The sectional force can be calculated with the calculation of stress for each layer. For the H100 and H120 series beams, tensile stresses were ignored in the calculation of the sectional force, but for the HF120 series beams, tensile stresses were considered in this calculation. The sum of the sectional forces in the whole layer must satisfy the equilibrium condition of the forces. The bending moment can be calculated based on the stress distribution along the cross section, satisfying the equilibrium condition of the forces.

The maximum bending moment from the test results and section analysis for each member is listed in Table 4. The ratio of the analyzed value to the measured value for the entire member was between 0.99 and 1.19, and the mean value of the ratios was 1.09. A simplified material law was adopted for the rebar by assuming horizontal linear behavior after the yielding point, as shown in Figure 16. In reality, the postyielding behavior of the rebar should be represented by a slightly ascending line resulting from the strain hardening of rebar. Both concrete and rebar contributed to the bending moment resistance. The compressive strength of the HSFRC was greater than that of the HSC, and the tensile strength of the HSFRC was also considered in integrating the stresses over the depth. This implies that, compared to concrete, the relative contribution of the rebar to bending moment capacity was lower in the HSFRC beams than in the HSC beams. Therefore, the consideration of strain hardening might lead to a greater difference between the prediction and test result of the bending moment for the HSC beams than for the HSFRC beams and to the underestimation of the

Table 4: Test and analytical results.

| Member | Bending strength | | Ratio (1)/(2) |
|---|---|---|---|
| | Test result (1) kN·m | Analytical result (2) kN·m | |
| H100-R1 | 57.2 | 50.6 | 1.13 |
| H100-R2 | 83.8 | 72.6 | 1.15 |
| H100-R3 | 104.8 | 94.2 | 1.11 |
| H120-R1 | 59.6 | 50.0 | 1.19 |
| H120-R2 | 79.3 | 71.6 | 1.11 |
| H120-R3 | 102.1 | 94.1 | 1.08 |
| HF120-R1 | 89.6 | 87.1 | 1.03 |
| HF120-R2 | 111.0 | 111.6 | 0.99 |
| HF120-R3 | 142.1 | 135.1 | 1.05 |
| Mean | | | 1.09 |

predicted bending moment for the HSC beams. The maximum bending moment of the HSFRC beams was more accurately estimated than those of the other series beams. Therefore, using this method to predict the bending strength was suitable for the HSFRC beams.

## 5. Conclusions

A comparative experimental study on the flexural behavior of HSFRC and HSC beams was carried out in this study. The following conclusions are drawn from the experimental results:

(1) The cracks propagated more deeply into the compressive zone in the HSC beam than in the HSFRC beam because the steel fibers arrested the crack propagation in the HSFRC beams. In addition, the crack width in the HSFRC beams was much smaller than that in the HSC beams.

(2) The failure of the HSC beams occurred by the sudden crushing of concrete in the compressive zone after the rebar yielded. On the other hand, the failure of the HSFRC beams typically resulted from the steel fiber pulling out of the concrete matrix along the major cracks.

(3) At the same rebar ratio, the crack stiffness of the HF120 series beams (HSFRC) was much greater than those of the H100 and H120 series beams (HSC). Therefore, the test results showed that the use of HSFRC significantly improved the crack stiffness of the concrete beams.

(4) The ductility index of the HSC beams decreased sharply with the increase in the rebar ratio. However, the ductility of the HSFRC beams slightly increased with the rebar ratio. In addition, HSFRC developed better and more consistent ductility with the increase of rebar ratio.

(5) The flexural toughness of the HSC beam was greater than that of the HSFRC beam at the low rebar ratio. However, the flexural toughness of the HSFRC beams was greater than that of the HSC beams at the higher rebar ratios. Therefore, the application of higher rebar ratios would be effective to improve the energy absorption capacity of HSFRC structures.

## Data Availability

The data used to support the findings of this study are available from the corresponding author upon request.

## Conflicts of Interest

The authors declare that they have no conflicts of interest.

## Acknowledgments

This research was financially supported by the Korean Ministry of Environment from the Public Technology Program Based on Environmental Policy (2016000700003). In addition, this research was supported by a grant (13SCIPA02) from the Smart Civil Infrastructure Research Program funded by the Ministry of Land, Infrastructure and Transport (MOLIT) of the Korean government and the Korea Agency for Infrastructure Technology Advancement (KAIA).

## References

[1] L. S. Hsu and C.-T. T. Hsu, "Complete stress-strain behavior of high strength concrete under compression," *Magazine of Concrete Research*, vol. 46, no. 169, pp. 301–312, 1994.

[2] T. H. Wee, M. S. Chin, and M. A. Mansur, "Stress-strain relationship of high-strength concrete in compression," *ASCE Journal of Materials in Civil Engineering*, vol. 8, no. 2, pp. 70–76, 1996.

[3] S. Sarkar, O. Adwan, and J. G. L. Munday, "High strength concrete: an investigation of the flexural behavior of high strength RC beams," *Structural Engineer*, vol. 75, no. 7, pp. 115–121, 1997.

[4] K. H. Min, H. C. Jung, J. M. Yang, and Y. S. Yoon, "Shrinkage characteristics of high-strength concrete for large underground space structures," *Tunneling and Underground Space Technology*, vol. 25, pp. 108–113, 2010.

[5] J. C. M. Ho, J. Y. K. Lam, and A. K. H. Kwan, "Effectiveness of adding confinement for ductility improvement of high-strength concrete columns," *Engineering Structures*, vol. 32, pp. 714–725, 2010.

[6] S. W. Shin, S. K. Ghosh, and J. Moreno, "Flexural ductility of ultra-high-strength concrete members," *ACI Structural Journal*, vol. 86, no. 4, pp. 394–400, 1989.

[7] M. A. Mansur, M. S. Chin, and T. H. Wee, "Flexural behavior of high-strength concrete beams," *ACI Structural Journal*, vol. 94, no. 6, pp. 663–674, 1997.

[8] S. A. Ashour, "Effect of compressive strength and tensile reinforcement ratio on flexural behavior of high-strength concrete beams," *Engineering Structure*, vol. 22, no. 5, pp. 413–423, 2000.

[9] M. A. Rashid and M. A. Mansur, "Reinforced high-strength concrete beams in flexure," *ACI Structural Journal*, vol. 102, no. 3, pp. 462–471, 2005.

[10] M. Mohammadhassani, S. Akib, M. Shariati, M. Suhatril, and M. M. A. Khanouki, "An experimental study on the failure modes of high strength concrete beams with particular references to variation of the tensile reinforcement ratio," *Engineering Failure Analysis*, vol. 41, pp. 73–80, 2014.

[11] P. Richard and M. Cheyrezy, "Composition of reactive powder concrete," *Cement and Concrete Research*, vol. 25, no. 7, pp. 1501–1511, 1995.

[12] B. A. Graybeal, "Material property characterization of ultra-high performance concrete," Tech. Rep. FHWA-HRT-06-103, FHWA, U.S. Department of Transportation, McLean, VA, p. 186, 2006.

[13] A. Abrishambaf, M. Pimentek, and S. Nunes, "Influence of fibre orientation on the tensile behaviour of ultra-high performance fibre reinforced cementitious composites," *Cement and Concrete Research*, vol. 97, pp. 28–40, 2017.

[14] S. T. Kang and J. K. Kim, "Investigation on the flexural behavior of HSFRCC considering the effect of fiber orientation distribution," *Construction and Building Materials*, vol. 28, pp. 57–65, 2012.

[15] H. Al-Mattarneh, "Electromagnetic quality control of steel fiber concrete," *Construction and Building Materials*, vol. 73, no. 30, pp. 350–356, 2014.

[16] B. Akcay and M. A. Tasdemir, "Mechanical behavior and fiber dispersion of hybrid steel fiber reinforced self-compacting concrete," *Construction and Building Materials*, vol. 28, no. 1, pp. 287–293, 2012.

[17] I. H. Yang, C. B. Joh, and B. S. Kim, "Flexural response predictions for ultra-high-performance fiber-reinforced concrete beams," *Magazine of Concrete Research*, vol. 64, no. 2, pp. 113–127, 2012.

[18] Q. Chunxiang and I. Patnaikuni, "Properties of high-strength steel fiber-reinforced concrete beams in bending," *Cement and Concrete Composites*, vol. 21, no. 1, pp. 73–81, 1999.

[19] J. Z. Su, B. C. Chen, and Q. W. Huang, "Experimental studies on the flexural behavior of HSFRC beams," in *Proceedings of AFGC-ACI-fib-RILEM International Symposium on Ultra-High Performance Fibre-Reinforced Concrete, UHPFRC*, Montpellier, France, October 2017.

[20] Q. Guan, P. Zhang, and X. Xie, "Flexural behavior of steel fiber reinforced high-strength concrete beams," *Research Journal of Applied Sciences, Engineering and Technology*, vol. 6, no. 1, pp. 1–6, 2013.

[21] H. C. Mertol, E. Baran, and H. J. Bello, "Flexural behavior of lightly and heavily reinforced steel fiber concrete beams," *Construction and Building Materials*, vol. 98, pp. 185–193, 2015.

[22] L. Chen and B. A. Graybeal, "Modeling structural performance of ultrahigh performance concrete I-girders," *Journal of Bridge Engineering*, vol. 17, no. 5, pp. 754–764, 2012.

[23] B. I. Bae, H. K. Choi, and C. S. Choi, "Flexural strength evaluation of reinforced concrete members with ultra high performance concrete," *Advances in Materials Science and Engineering*, vol. 2016, Article ID 2815247, 10 pages, 2016.

[24] X. Ning, Y. Ding, F. Zhang, and Y. Zhang, "Experiment study and prediction for flexural behavior of reinforced SCC beam containing steel fibers," *Construction and Building Materials*, vol. 93, pp. 644–653, 2015.

[25] RILEM TC 162-TDF, "Test and design methods for steel fiber reinforced concrete; bending test-final recommendation," *Material and Structures*, vol. 35, no. 253, pp. 579–582, 2002.

[26] T. H. K. Kang, W. Kim, Y. K. Kwak, and S. G. Hong, "Flexural testing of reinforced concrete beams with recycled concrete aggregates," *ACI Structural Journal*, vol. 111, no. 3, pp. 607–616, 2014.

[27] M. Singh, A. H. Sheikh, M. S. Mohamed Ali, P. Visintin, and M. C. Griffith, "Experimental and numerical study of the flexural behaviour of ultra-high performance fibre reinforced concrete beams," *Construction and Building Materials*, vol. 138, pp. 12–25, 2017.

[28] I. H. Yang, C. Joh, and B. S. Kim, "Structural behavior of ultra high performance concrete beams subjected to bending," *Engineering Structures*, vol. 32, pp. 3478–3487, 2010.

[29] A. N. Dancygier and Z. Savir, "Flexural behavior of HSFRC with low reinforcement ratios," *Engineering Structures*, vol. 28, pp. 1503–1512, 2006.

[30] L. Biolzi and S. Cattaneo, "Response of steel fiber reinforced high strength concrete beams: experiments and code predictions," *Cement and Concrete Composites*, vol. 77, pp. 1–13, 2017.

[31] AFGC, *Ultra High Performance Fibre-Reinforced Concretes*, Association Française de Génie Civil (AFGC), Paris, France, 2013.